Numerical Simulation of Subfields in a Multi-Tower Concentrated Solar Field

Zaharaddeen Ali Hussaini[1] iD, Christopher Sansom[1] iD, Peter King[2] iD, and Mounia Karim[1] iD

[1]University of Derby, UK

[2]Cranfield University, UK

*Correspondence: Zaharaddeen Ali Hussaini, z.hussaini@derby.ac.uk

Abstract. The research introduces an innovative approach to enhancing the efficiency of Multi-tower Concentrated Solar Power (CSP) through a configuration termed Auxiliary Tower with Subfield (ATS). ATS introduces an auxiliary tower and creates a subfield by adding heliostats near its position, aiming to optimize the solar field's optical efficiency and offer modular decentralized power output. ATS configuration employs existing field configurations to pinpoint inefficiencies where an additional tower can be installed, and heliostats are systematically added to the subfields through numerical optimization using various design variables. Although the inclusion of a subfield in the ATS configuration enhances energy output, it does not always offset the additional costs of the auxiliary tower, receiver, and extra heliostats, in small fields. However, when applied to larger fields, starting from 200MWth, ATS begins to provide a lower Levelized Cost of Heat (LCOH) compared to optimized conventional thermal fields, demonstrating its potential applicability and efficiency in larger-scale CSP setups. Applying ATS to a 120 MWth Gemasolar-like plant further confirms its advantages, with 160 MWth emerging as the optimal enhancement point that boosted efficiency while lowering LCOH. ATS shows promise as an efficient, modular approach to scaling up power tower system.

Keywords: Multi-Tower CSP, Modular Power Tower, Tower CSP Optimization

1. Introduction

The exploration and development of multi-tower setups within Concentrated Solar Power (CSP) systems have garnered increased attention, both historically and in more contemporary research, as the transition toward distributed energy systems becomes ever more important. Historically, innovative models like Romero et al.'s Modular Integrated Utility Systems (MIUS) have underscored the advantages of decentralized energy, advocating for smaller, integrated tower fields [1]. This trajectory continued with the Multi-Tower Solar Array (MTSA) system, introduced by Schramek and Mills, which investigated the concept of heliostat overlapping in multi-tower contexts to maximize solar radiation use [2]. Methodologies enabling individual heliostats to aim at designated receivers in a multi-tower configuration, adhering to a specific aim selection criterion, were presented by Augsburger and Favrat, providing a lens into the thermo-economic viability of multi-tower fields [3]. The transition from theoretical models to operational prototypes are exemplified by Vast Solar's modular solar array field [4]. These developments highlight the sector's potenital, marked by the Three Gorges Renewables' on-going dual tower CSP project [5]. Recent studies have further enriched multi-towers and moular towers, with research emphasizing both optimization and economic feasibility. For instance, enhanced optical efficiency in CSP plants [6], applications of advanced computational methods

for system layout optimization [7], and promising economic forecasts for multi-tower CSP plants [8], [9] collectively underscore the increasing potential of multi and modular towers.

The present study builds on previous work by authors on multi-tower CSP feasibility [10], this paper introduces a multi-tower with multi-aim approach titled Auxiliary Tower with Subfield (ATS). In ATS, heliostats are added near the position of the auxiliary tower, thereby creating another region in the field, referred to as a subfield. The configuration shares similarities with much of the literature on multi-tower setups, which have a surrounding field for each tower. However, ATS is unique in that it develops a subfield complementary to a multi-tower setup with multi-aiming capability. The auxiliary towers in ATS act as targets for both the weak heliostats in the main field and the newly added heliostats in the subfield. The paper details ATS field layout, aiming methodology, and performance optimization. Results show ATS can improve efficiency and cost-effectiveness over conventional CSP plants, but only at large scales.

2. Auxiliary Tower with Subfield (ATS) configuration

The Auxiliary Tower with Subfield model distinctively marries a conventional CSP field (main field) and an auxiliary tower with additional heliostats to create a subfield, expanding the power-generating capacity while addressing potential weak spots in the field [10]. By placing the auxiliary tower and introducing a subfield, ATS enhances the solar field's optical efficiency, redirecting weak heliostats in the main field and the newly added ones to augment the overall energy incident on the receiver. Auxiliary towers in ATS not only serve as the additional targets for heliostats but also facilitate the multi-aim approach, enabling each heliostat to direct sunlight to either the main or auxiliary tower depending on optimal solar capture. All heliostats in the field (subfields inclusive) are arranged using the radial staggered field layout. To achieve this, the Campo method is adopted in this work [11]. A depiction of the ATS configuration in a one and two auxiliary tower configuration is shown in Figure 1.
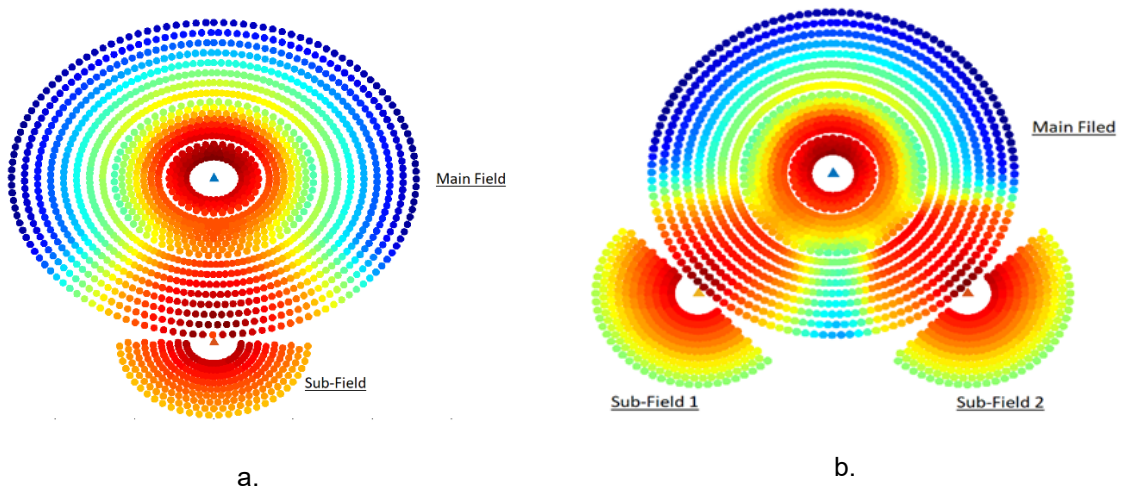

a.   b.

Figure 1 a. *One ATS configuration set-up showing main filed and sub-field* **b.** *Two ATS configuration set-up showing the two subfields and the main field*

The heliostat layout methodology in ATS starts with a compact arrangement, deploying concentric rows of heliostats. Parameters defining the field layout, curled from Collado's Campo algorithm, are illustrated in Figure 2.
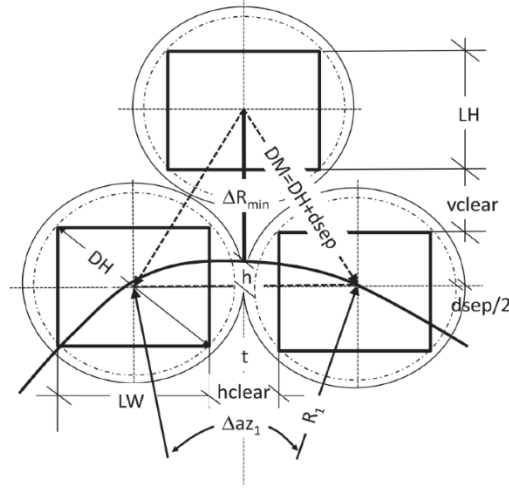
Figure 2. *Parameters of the field layout*

Heliostats within each row are positioned at a radius R_1 from the central tower, separated by an azimuth angle Δaz_1, as shown in equation (1):

$$\Delta az_1 = 2\sin^{-1}\left(\frac{DM}{2R1}\right) \tag{1}$$

where R_1 is defined by the number of heliostats in the row $Nhel_1$:

$$R_1 = Nhel_1\left(\frac{DM}{2\pi}\right) \tag{2}$$

New zones in the field are established when the spacing between heliostats becomes larger than the horizontal clearance, DM. Both the main field and subfields in the ATS configuration is restricted to three zones. The radius for subsequent zones (i) is calculated using equation (3):

$$R_1 = 2^{i-1}\left(\frac{DM}{\Delta az_1}\right) \tag{3}$$

Auxiliary towers placement distance (A_t) in the multi-tower configuration are defined by:

$$A_t = (dsep \times DM) + D_f \tag{4}$$

where D_f is the final distance between the central tower and the furthest heliostat in the same axis direction of the auxiliary tower location. The range of values for $dsep$ is set between 0.866 and 1.066. The methodology for developing multi-tower configurations has been elaborated in greater detail in [10] by the authors.

Heliostats in the subfield are developed using the same methodology and guided by equations (1)-(4) with the auxiliary tower position taken as the central position of the new heliostats. Heliostats in the subfields in this setup are constrained to the southern region of the auxiliary tower within a 180° angle. The heliostats in both the main field and subfields are not restricted by which tower they are allowed to focus on. Each heliostat decides on the receiver to aim at based on the strength of the reflected radiation determined by the aim point bearing the lesser optical efficiency loss.

Design variables of the field are optimized using Genetic Algorithm (GA), with the objective function being the Levelized Cost of Heat (LCOH) of an independent generating system (equation (5)). The LCOH in ATS is compared to a conventional field of a similar thermal rating.

The model assumes 100% conversion of incident energy on the receiver's surface. Further details are highlighted in the following section. The ATS model is developed using Mathwork's MATLAB.

$$LCOH = \frac{Heliostat\ Field\ Cost}{Thermal\ Output\ at\ Reciever's\ Surface} \tag{5}$$

ATS configuration is initially applied in an optimised and conventional 50MWth field. The designated site, situated in the northern hemisphere, has an annual direct solar energy availability of 1,612 kWh/m^2/year. The methodology, along with the computational details of the design variables for the conventional 50 MWth field, has once again been highlighted in a previous work by the authors [10]. Summary of results from this conventional field are re-presented in Table 1.

Table 1. *Summary of Key results from 50MWth conventional power tower field*

Parameter	Value
Heliostat Area	95.17 m^2
Central Tower Height	91.48 m
Central Receiver Area	55.84 m^2
Levelized Cost of Heat, LCOH	0.0473 $/kWht
Power	49.89 MWth
Efficiency Design Point	60.59 %
Mean Annual Efficiency	55.63 %
Reflective Surface Area	152,270 m^2
Annual Energy	151,849 MWht
System Cost ($)	$ 40,652,834

2.1 One ATS configuration

The One ATS configuration employs just one additional tower, around which a subfield of heliostats laid out. In implementing the One ATS configuration, specific design variables are crucial in the strategic placement and sizing of components, particularly concerning the heliostats and the auxiliary tower. These variables for the subfield, which influence the system's optical performance and the efficiency of energy capture, are outlined with their permissible ranges in Table 2.

Table 2. *PTC Design specification*

Design Variables	Variable Range
Heliostat Row Separation Distance in subfield (m)	(0.866 – 1.066) × DM*
Auxiliary Tower Placement Distance (m)	((0.866 – 1.066) × DM) + Df**
Auxiliary Tower Height (m)	40 – 140
Auxiliary Tower Receiver Dimensions (m^2)	6 – 80

In the methodology for this configuration, heliostats are systematically incorporated into the subfield through numerical optimization, employing the various design variables. Consistently, the heliostat area across all fields is maintained. For the 50 MWth field, the maximum number of heliostats that can be introduced into the subfield is capped at the original quantity in the main field, which is 1,600. This constraint not only prevents the subfield from surpassing the main field in size but also mitigates the computational load.

3. Results and discussions

3.1 One ATS configuration

Figures 3a-d illustrate the computational results, showing the impact of incrementally integrating heliostats into the auxiliary tower's subfield across various parameters using all the design varibles highlighted in Table 1.
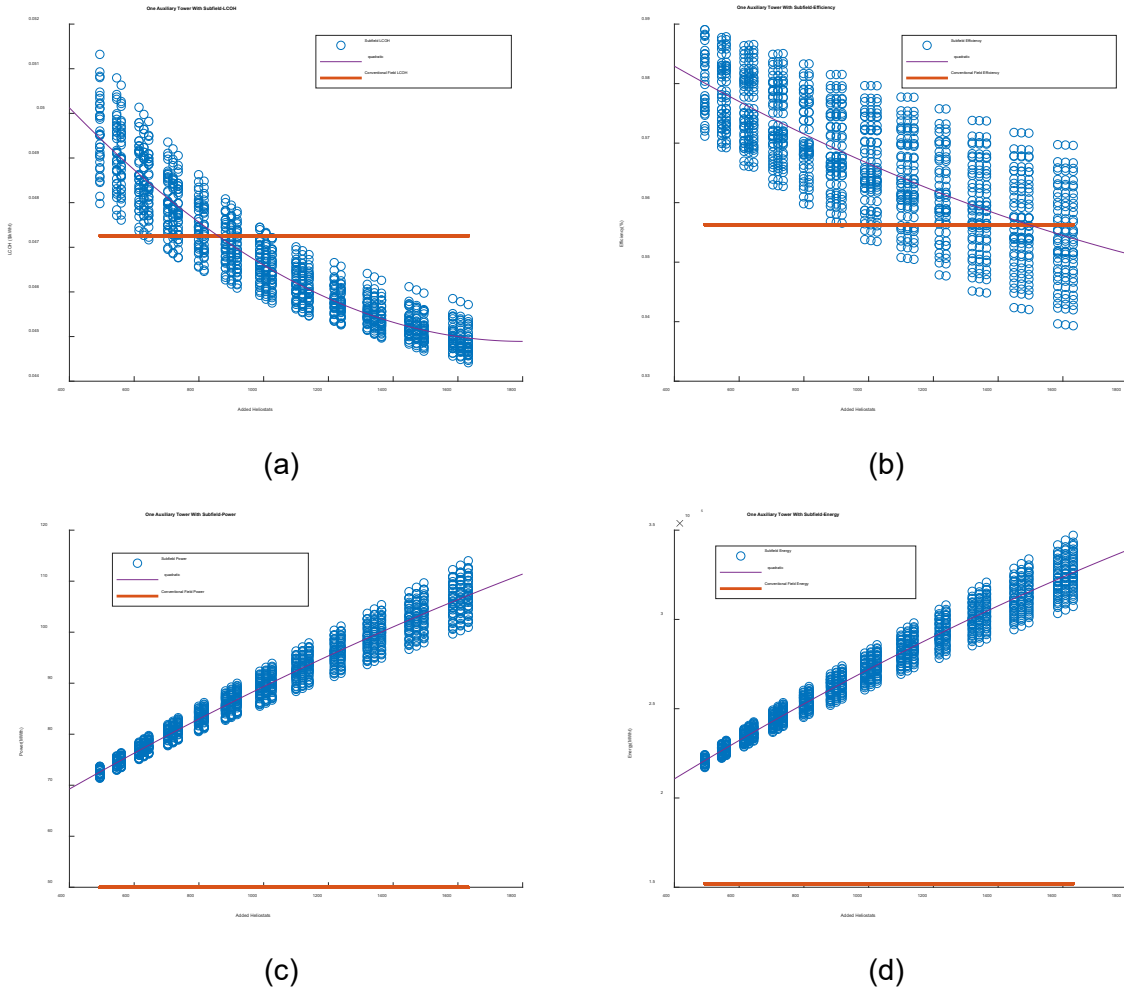

(a)   (b)

(c)   (d)

Figure 3. *Computational results showing the effect of ATS for different parameters **a.** LCOH **b.** Mean annual efficiency **c.** Field thermal power **d.** Annual thermal energy*

In Figure 3a, the trend of the LCOH can be seen with a varying number of heliostats added onto the subfield. As the heliostats are added, an improvement in the LCOH is continuously observed within the limits of the 1,600-maximum number of added heliostats in the subfield. Notably, beyond the 1,100th heliostat, the LCOH's rate of decrease begins to taper off. The graph pinpoints an optimization crossroad at the 855th heliostat, where the ATS configuration yields superior LCOH values compared to the conventional setup. This economic advantage is sustained, as evidenced at the 1,088th marker, where all subsequent LCOH readings outperform the traditional 50MWth field.

Figure 3b, presents a comparison of the conventional field's mean annual efficiency (at a value of 55.63%) against the varying efficiencies achieved within the ATS setup. At the 988th heliostat, the ATS starts to achieve lower efficiency values. This decrease continues as more heliostats are added mainly because of the increase in the optical losses incurred as heliostats

in the subfield move further away from the auxiliary tower. The mean efficiency value can serve as a good indicator as to which point the addition of heliostats in the subfield can be stopped.

Figure 3c&d provide the thermal field power, and energy outlook of the field as heliostats are added into the subfield. As more heliostats are added, a steady increase in the power and annual field energy is observed. At all the points of added heliostats considered, the configuration provides a higher value of both the energy and power when compared to the conventional field.

3.2 Analysis of ATS and conventional configurations.

While the ATS configuration contributes significant improvements in field performance, its outcomes aren't directly comparable to those of a conventional 50MWth field. This distinction stems from the interconnected nature of the added heliostats with variables like thermal field power and energy, detailed in Figure 3. For instance at a thermal field power of 75MWth in a 50MWth One ATS field, the optimal LCOH is obtained at 0.0479$/kWht by adding 615 heliostats to the subfield. However, a conventional 75MWth field holds a marginally better LCOH at 0.0463$/kWht. Despite the ATS configuration's increased thermal power output (from 50MWth to 75.21MWth) and the 1.07% improvement in mean field efficiency from 55.63%, the conventional field retains a more favorable LCOH. This discrepancy indicates that the supplementary costs implicated in the ATS configuration, including an extra tower, additional heliostats, and expanded receiver apparatus, fail to compensate for the theoretical benefits presented by this system for a 50MWth field under the given incident DNI. Figure 4 provides a visual comparison, illustrating the layouts of both a conventional 50MWth field and a 75MWth field utilizing a single ATS configuration.
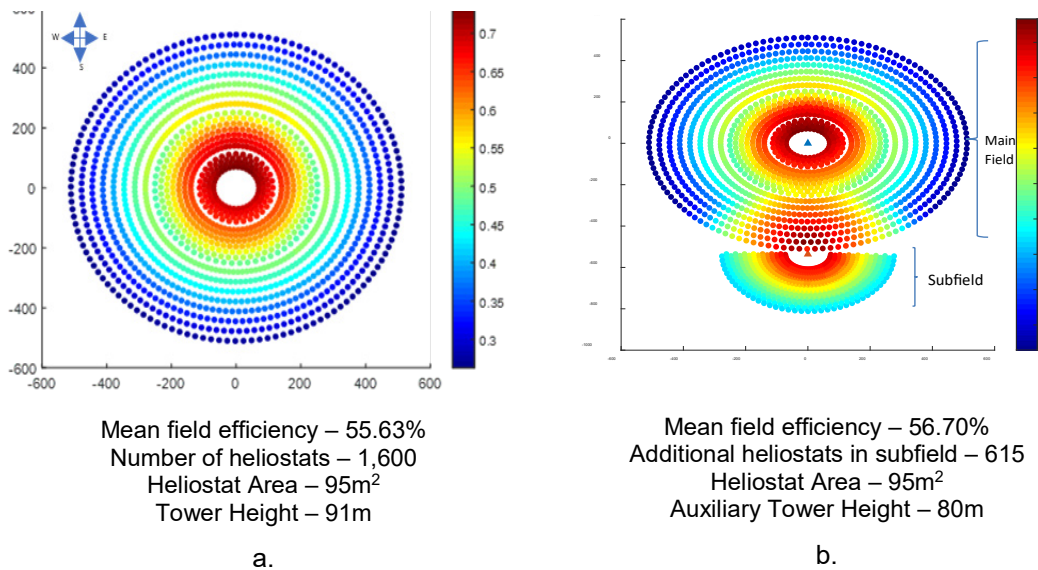

Mean field efficiency – 55.63%
Number of heliostats – 1,600
Heliostat Area – 95m^2
Tower Height – 91m

a.

Mean field efficiency – 56.70%
Additional heliostats in subfield – 615
Heliostat Area – 95m^2
Auxiliary Tower Height – 80m

b.

Figure 4 a. *50MWth conventional field layout.* **b.** *One ATS configuration showing the layout of 75MWth thermal field*

To further investigate the role ATS has, larger field size is considered. Figure 5 shows the LCOH for conventional fields and One ATS configuration at different thermal powers.
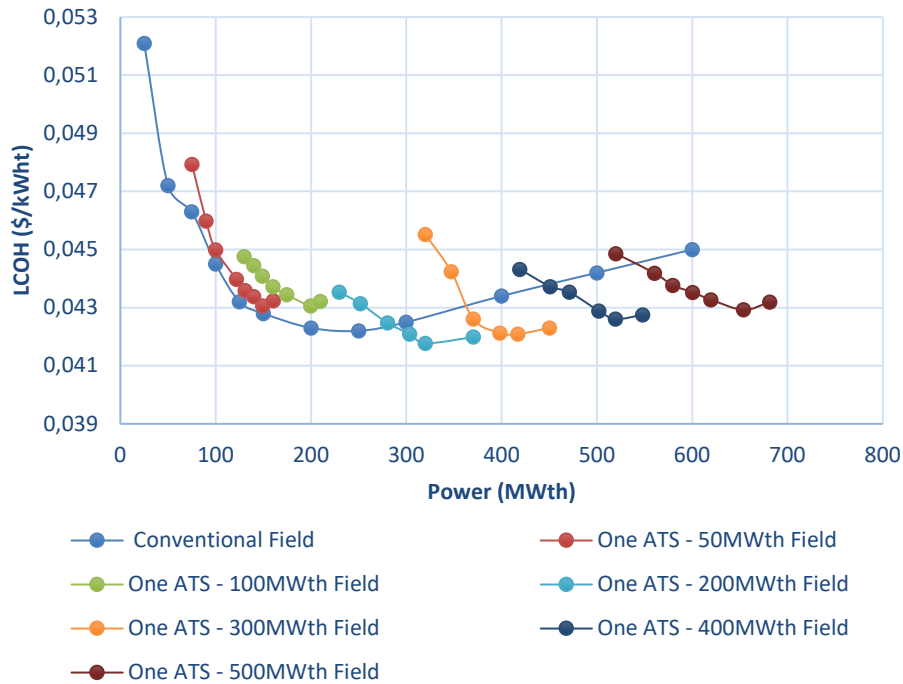
Figure 5. *LCOH for conventional field and one ATS configuration at different thermal*

Focusing initially on 50MWth conventional field, despite the ATS configuration enhancing the energy output due to the additional subfield, this increase doesn't translate into a superior LCOH compared to conventional fields. The heightened costs associated with the extra tower, receiver, and additional heliostats negate the advantages brought by the increased energy yield.

Looking at other thermal power in Figure 5 reveal that the cost-effectiveness of the ATS configuration significantly improves as the scale of the field increases. This advantage becomes evident in multi-tower fields with capacities starting from fields from 200MWth One ATS. Here, the ATS configuration begins to show a more favourable LCOH compared to conventional fields, with this trend growing notably around 300MWth. This improvement continues until 370MWth when the downward trend begins to change, highlighting an optimal range for ATS efficiency.

In the context of larger operations, the ATS configuration achieves lower LCOH values across a wide range of thermal powers, particularly in fields with substantial capacities of 300MWth, 400MWth, and 500MWth, the ATS model maintains an advantage, delivering improved LCOH for extended thermal power ranges.

The ATS configuration underscores a trade-off. While introducing additional complexities and costs in smaller setups, such as the 50MWth fields, its value becomes increasingly apparent in larger-scale applications, reaching optimal cost-effectiveness and efficiency at higher upper thermal power levels.

3.3 Application of ATS in a Gemasolar-like field

The Gemasolar plant is the first commercial solar power tower plant supplying grid electricity to over 25,000 homes featuring a molten salt receiver with thermal storage capabilities [12]. The plant has a nominal output of 19.9MWe with up to 15 hours thermal energy storage. In this section, the One ATS configuration is applied to Gemaolsr-like field. Table 3 summarises

the parameters for a Gemasolar-like field modelled sing MATLAB. Technical specification of the real plant is followed where data is available.

Table 3. *Developed Gemasolar plant parameters model*

Parameter	Gemasolar-like Model
Heliostat Area	115.25 m^2
Central Tower Height	140 m
Central Receiver Area	384.24 m^2
Annual Direct Solar Energy	2,534 kWh/ m^2/year
Reflective Surface Area	305,402 m^2
Number of Heliostats	2,650
Annual Direct Solar Energy	774,020.32 MWht
Mean Field Efficiency	51.22 %
Levelized Cost of Heat, (LCOH)	0.0449 $/kWht
Receiver Thermal Power	120.68 MWth
Annual Incident Receiver Energy	396,453 MWht
System Cost ($)	$ 97,025,168

Table 4 shows the resulting metrics upon the ATS's integration into the Gemasolar-like model.

Table 4. *Auxiliary Tower with Subfield results at optimum levelized Cost of Heat for different overall field thermal powers in a Gemasolar field*

Total Field Thermal Power (MWth)	Annual Power at Auxiliary Receiver (MWth)	Annual Energy at Auxiliary Receiver (MWht)	Optimum Levelized Cost of Heat ($/MWht)	Total Field Energy (MWht)	Mean Annual Field Efficiency (%)	Total Field Reflective Surface Area (m^2)
120.68 (Initial Gemasolar Field)	-	-	0.0449	396,453	51.22	305,402
139.37	18.69	64,575	0.0454	465,380	50.90%	353,805
160.10	41.12	147,351	0.0440	547,916	51.79%	409,123
179.50	60.62	225,024	0.0429	625,546	50.75%	477,695
199.68	82.05	303,231	0.0419	703,556	50.68%	538,775
221.17	104.72	386,149	0.0412	786,279	50.41%	609,075
239.12	121.49	460,126	0.0410	860,451	48.92%	720,288

From Table 4, a Lower LCOH (0.0440 $/MWht) from the initial field is only attained when 420 heliostats are added onto the field at the 160MWth mark. In the subsequent thermal field sizes, the LCOH's diminishing rate of decrease points to a consequential efficiency drop in the field, caused primarily in the subfield as more heliostats are added.

The total reflective surface area from Table 4 shows a progressive increase in the relative surface area at the field's thermal powers. This metric is illustred better in Figure 6.
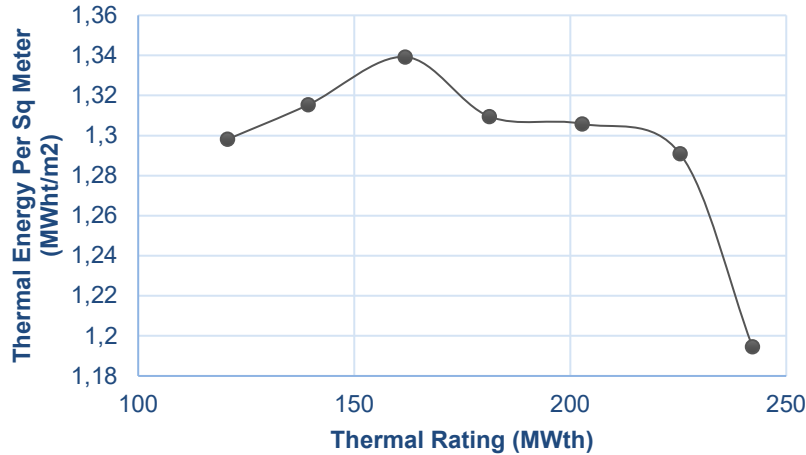
Figure 6. *Thermal energy per square meter attained in the Auxiliary Tower with Subfield configuration*

Figure 6 illustrates the thermal energy yield per square meter with varying field powers. Initially, up to 140MWth, energy gain outpaces area increase. However, beyond 220MWth, the larger reflective area no longer translates to proportional energy gains. The data points to an efficiency peak at 160MWth, where additional heliostats contribute more energy relative to the increase in area. This suggests 160MWth as the optimal point for enhancing the Gemasolar field with the ATS system.

4. Conclusion

This study introduces an innovative Auxiliary Tower with Subfield (ATS) configuration for enhancing the efficiency and modularity of multi-tower concentrated solar power systems. The ATS model employs an auxiliary tower with an adjoining subfield of systematically added heliostats to improve solar capture and allow multi-aiming flexibility.

Results indicate the ATS configuration can achieve higher thermal power output and improved optical efficiency compared to conventional multi-tower layouts. However, the additional components involved fail to make ATS more cost-effective for smaller 50 MWth fields. The benefits of ATS become more apparent for large-scale applications above 200 MWth, where the configuration attains superior levelized cost of heat over extended thermal power ranges, with optimal efficiency around 300-400 MWth.

Applying ATS to a Gemasolar-like plant further confirms its advantages for sizable operations, with 160 MWth emerging as the optimal enhancement point where a lower LCOH is registered with a higher mean field efficiency.

ATS shows promise as an efficient, modular approach to scaling up power tower systems, particularly for large thermal fields. Further analysis into optimizing heliostat fields and aiming strategies can help maximize performance. The decentralized, complementary nature of ATS also promotes adaptable and incremental capacity growth aligned with distributed energy priorities.

Data availability statement

The authors confirm that the data supporting the findings of this study are available within the article. Additional information on data can be made available upon reasonable request from the corresponding author.

Author contributions

Zaharaddeen Ali Hussaini: Conceptualization; writing – original draft; formal analysis; Investigation. Christopher Sansom: Supervision; formal analysis; project administration; writing – review and editing. Peter King: Investigation; project administration; formal analysis. Mounia Karim: Resources; writing – review and editing.

Competing interests

The authors declare that they have no competing interests.

References

1. Romero, M., Marcos, M. J., Téllez, F. M., Blanco, M., Fernández, V., Baonza, F., & Berger, S. (1999). Distributed power from solar tower systems: A MIUS approach. Solar Energy, 67(4–6), 249–264. https://doi.org/10.1016/s0038-092x(00)00059-1
2. Mills, D., Schramek, P., Dey, C., Buie, D., Imenes, A., Haynes, B., & Morrison, G. (2002). Multi Tower Solar Array Project. ANZSES Annual Conference—Solar Harvest, November 2015, Paper 1b4.
3. Augsburger, G., & Favrat, D. (2012). From Single- to Multi-Tower Solar Thermal Power Plants: Investigation of the Thermo-Economic Optimum Transition Size. Proceedings of the SolarPACES 2012 Conference on Concentrating Solar Power and Chemical Energy Systems.
4. Wood, C., & Drewes, K. (2019). Vast Solar: improving performance and reducing cost and risk using high temperature modular arrays and sodium heat transfer fluid. Proceedings of the SolarPaces Conference, 1–4.
5. SolarPaces. (2023, June 14). Three Gorges' new Chinese CSP project tries a double solar field. SolarPaces. https://www.solarpaces.org/new-chinese-csp-project-three-gorges-renewables-trials-double-solar-field/
6. Serrano-Arrabal, J., Serrano-Aguilera, J. J., & Sánchez-González, A. (2021). Dual-tower CSP plants: optical assessment and optimization with a novel cone-tracing model. Renewable Energy, 178, 429–442. https://doi.org/10.1016/j.renene.2021.06.040
7. Pisani, L., Moreau, G. S., Leonardi, E., Podda, C., Mameli, A., & Cao, G. (2023). Multi-tower heliostat field optimization by means of adiabatic quantum computer. Solar Energy, 263. https://doi.org/10.1016/j.solener.2023.111893
8. Buck, R., & Sment, J. (2023). Techno-economic analysis of multi-tower solar particle power plants. Solar Energy, 254, 112–122. https://doi.org/10.1016/j.solener.2023.02.045
9. Rovense, F., Reyes-Belmonte, M. Á., Romero, M., & González-Aguilar, J. (2022). Thermo-economic analysis of a particle-based multi-tower solar power plant using unfired combined cycle for evening peak power generation. Energy, 240. https://doi.org/10.1016/j.energy.2021.122798
10. Hussaini, Z. A., King, P., & Sansom, C. (2020). Numerical simulation and design of multi-tower concentrated solar power fields. Sustainability (Switzerland), 12(6), 13–16. https://doi.org/10.3390/su12062402
11. Collado, F. J., & Guallar, J. (2012). Campo: Generation of regular heliostat fields. Renewable Energy, 46, 49–59. https://doi.org/10.1016/j.renene.2012.03.011
12. Burgaleta JI., Arias S., Ramirez D. Gemasolar: The First Tower Thermosolar Commercial Plant with Molten Salt Storage System. SolarPACES International Conference. 2012; (Sept.): 11–14